IEEE Photonics Journal
An IEEE Photonics Society Publication

Computational Analysis of the Power Spectral Shifts and Widths Along Dye-Doped Polymer Optical Fibers

Volume 2, Number 3, June 2010

J. Arrue
F. Jiménez
M. A. Illarramendi
J. Zubia
I. Ayesta
I. Bikandi
A. Berganza

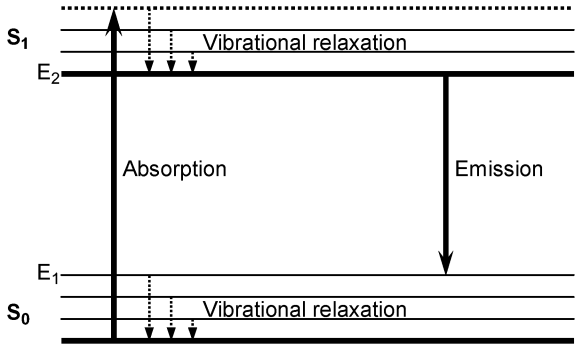

DOI: 10.1109/JPHOT.2010.2050196
1943-0655/$26.00 ©2010 IEEE

Computational Analysis of the Power Spectral Shifts and Widths Along Dye-Doped Polymer Optical Fibers

J. Arrue, F. Jiménez, M. A. Illarramendi, J. Zubia, I. Ayesta, I. Bikandi, and A. Berganza

Escuela Técnica Superior de Ingeniería de Bilbao, University of the Basque Country, UPV/EHU, 48013 Bilbao, Spain

DOI: 10.1109/JPHOT.2010.2050196
1943-0655/$26.00 ©2010 IEEE

Manuscript received April 20, 2010; revised May 4, 2010; accepted May 5, 2010. Date of publication May 12, 2010; date of current version June 15, 2010. This work was supported by Ministerio de Ciencia e Innovación, University of the Basque Country UPV/EHU, Gobierno Vasco/Eusko Jaurlaritza, and the European Commission's 7th Framework Program (FP7), under Projects TEC2009-14718-C03-01, GIU05/03 and UE08-16, AIRHEM and S-PE09CA03, and AISHAII, respectively. This work was also supported by the European Commission's Seventh Framework Program [FP7/2007-2013] under Grant agreement no. 212912. Corresponding author: J. Arrue (e-mail: jon.arrue@ehu.es).

Abstract: Polymer optical fibers doped with organic dyes can be used as efficient optical amplifiers and lasers in the visible region. We computationally analyze the spectral features of both their fluorescence and their amplified emission for different amounts of overlap between the emission and absorption spectra of the dyes employed. Representative cases are compared by calculating the respective evolutions along the doped fiber of the average wavelength, peak wavelength, and full-width at half-maximum of the output power obtained.

Index Terms: Fiber optical amplifiers, fiber lasers, polymer optical fibers, dye lasers.

1. Introduction

Polymer optical fibers (POFs) have raised great interest in applications such as local area networks and sensors and, more recently, also in the field of fiber lasers and amplifiers in the visible region when they are doped [1]–[5]. The lower manufacturing temperatures of POFs, as compared with glass fibers, make it possible to embed both organic and inorganic dopant materials in the fiber, which has been the subject of incipient research. An important issue is that organic dyes present extremely large absorption and emission cross sections in comparison with those of Er^{3+} ions, which are commonly employed in glass [6]. Such dyes can be easily dissolved in the main material employed for the POF core, namely polymethyl methacrylate (PMMA), but not in silica glass. Organic dyes combined with POFs allow a reduction of the fiber laser/amplifier length from a few meters to a few centimeters or even shorter.

One of the aspects that are being investigated is the spectral shift with distance of the emission power of active POFs doped with organic dyes, which can be employed for making tunable fiber lasers and amplifiers [7]–[9]. Specifically, the emission and absorption cross sections can change significantly from one dopant to another, thus allowing the designer the chance of amplifying at any wavelength of interest in a broad spectral range. The highest gain usually appears in the proximity of the emission spectrum peak [10], [11]. However, when the emission and absorption cross sections overlap significantly, the absorption of the fiber can have a strong influence on the output spectrum, which can present a shift either toward longer or toward shorter wavelengths (i.e., "red

shift" or "blue shift", respectively). After some degree of red shift has taken place, further blue shifts can be interpreted as reductions in the red shift from the original situation. Such shifts will be called relative blue shifts.

The spectral shifts depend on the pump power and on the fiber length [8], [12]. This is an important issue, because the emission spectrum from a pumped active POF provides information about the range of wavelengths that can be amplified in it when used as a fiber laser or as a fiber amplifier. Note that a simple fiber laser without mirrors can emit a laser-like light. This process is often called Amplified Spontaneous Emission (ASE) or mirrorless lasing. The light presents many of the properties of laser radiation, such as a threshold, a narrower linewidth, and directionality. However, these properties are less developed than in a laser with mirrors due to the absence of a resonator [13], [14].

In this paper, we spectrally analyze the emission of doped POFs below and above the threshold. We also show to what extent it is possible to tune the spectral emission of active POFs by changing the fiber length. One of the novelties of our work is that the spectral study is made computationally for the first time, as far as we know. We pay special attention to the influence of the overlap between the emission and absorption curves that characterize the dopant, although the computational method developed could serve for many other types of analyses, even in the time domain as well. For the analysis, POFs are pumped with short light pulses of several energies, from low energies yielding fluorescence emissions to high ones above threshold. The analysis above threshold can serve to tune the spectral gain of an active POF by changing the fiber distance traveled by the pump power [7]–[9]. Even below threshold, the analysis could be useful for several applications, e.g., for measuring the absorption of a doped POF without having to cut it and for the characterization of losses as a function of the POF length [3], [12].

By using our model, we analyze the spectral behavior of active PMMA POFs doped with two different types of dopant regarding the overlap between absorption and emission. One of the dopants is the well known rhodamine B, which has a large overlap between emission and absorption, and the other is the conjugated polymer poly(9,9-dioctylfluorenyl-2,7-diyl) (also called PFO), which has a small overlap. The latter is a type of dopant that is particularly interesting nowadays. Conjugated polymers show little concentration quenching and great fluorescence efficiencies. Besides, they can offer advantages in terms of the higher photoluminescence yield achievable and the future possibility of electrical excitation, although the new ones that are being investigated as dopants are optically pumped [15]. For the computational calculations, the emission and absorption cross sections are needed. These provide information about the probabilities of the possible electronic transitions that give rise to photon emission and absorption. The emission cross section of rhodamine B has been measured and reported by other authors [6], [7], [16], [17]. The absolute values can be found in [16]. In the case of PFO, we measured the fluorescence curve to determine the shape of the emission cross section, and we calculated the absolute values by normalizing according to the corresponding value reported in the literature [18]. Regarding the spectrum emitted from a doped POF, the peak wavelength can be strongly influenced by the absorption curve of the dopant and by the fiber distance.

This paper is organized as follows. The theoretical and computational analysis of the emission of active POFs is explained in Section 2. Experimental results are presented and compared in Section 3. This helps to understand the choice of the dopants analyzed. The shifts in the emission spectra with traveled distance are explained in Section 4. We also show that the spectral shifts are usually accompanied by significant changes in the spectrum width. The evolution of the spectrum width with distance can have very different behaviors depending on the pump power and on the type of dopant. The respective evolutions along the doped fiber of the average wavelength (λ_{av}), peak wavelength (λ_{peak}) and full-width at half-maximum (FWHM) of the generated spectral power are obtained for several different pump powers. The conclusions are summarized in Section 5.

2. System Model and Numerical Scheme

We will start with a brief description of the most important optical transitions in the dopants employed. Organic dyes have two main electronic energy states S_0 and S_1, with many energy vibrational levels within each one of them [15]. Transitions between vibrational levels within each

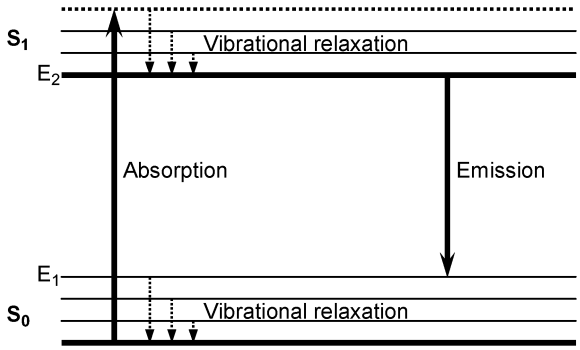

Fig. 1. Energy levels in organic dyes responsible for photon absorption and emission.

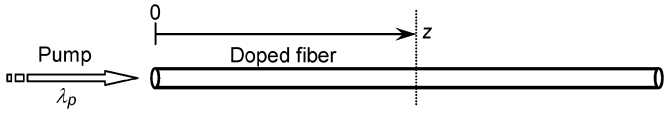

Fig. 2. Setup for the calculation of the spectral features of light as it propagates in a doped POF.

electronic energy state are very rapid and nonradiative, in such a way that most of the population within each of the two main energy states at any given time is at its corresponding ground level. Therefore, photon emissions occur from the ground level of state S_1 to one of the vibrational energy levels of state S_0, while photon absorptions occur from the ground energy level of state S_0 to one of the vibrational energy levels of state S_1. This is shown in Fig. 1.

The optical properties in the doped fiber are usually analyzed by means of time-dependent rate equations between two main energy levels (E_1 and E_2) [16]. In our analysis, the independent variables are not only the time t and the position z measured along the fiber symmetry axis (see Fig. 2), but the wavelength λ as well. The only spatial variable is z because the fiber cross sections are much smaller than the fiber lengths. We consider the case that the doped POF is pumped from one end with approximately monochromatic light (see Fig. 2). When the aim is to carry out a spectral analysis of the light power, it is necessary to consider its dependence on the wavelength as well, i.e., $P(t, z, \lambda)$. To introduce this dependence, we make use of the λ-dependent absorption and emission cross sections $\sigma^a(\lambda)$ and $\sigma^e(\lambda)$ of the dopant, and we divide the range of wavelengths of interest into discrete subintervals centered at wavelengths λ_k.

The complete system is described by a set of partial differential equations, initial conditions and boundary conditions. The unknown functions to be determined are P (light power) and N_2 (electronic population in the excited level E_2). We also take into account the rather trivial relationship $N_1 = N - N_2$ between N_2 and the population N_1 in level E_1, where N is the dopant concentration. Besides, three differential equations are employed. The following equation governs the evolution of the pump power P_p:

$$\frac{\partial P_p}{\partial z} = -\sigma^a(\lambda_p) N_1 P_p - \frac{1}{c/n}\frac{\partial P_p}{\partial t}. \tag{1}$$

The first right-hand term in (1) represents the absorption of the pump. The product $\sigma^a(\lambda_p)N_1$ is the absorption coefficient α_p of the material at λ_p. The increase of N_2 due to the pump reduces N_1, and thus, the absorption coefficient decreases in the presence of pump power. The last term in (1) represents the propagation of the pump.

The variation of N_2 with time at a given point is governed by

$$\frac{\partial N_2}{\partial t} = \frac{-N_2}{\tau} - \left(\frac{\sigma^e(\lambda_k)}{h(c/\lambda_k)A_{core}}\right) N_2 P + \left(\frac{\sigma^a(\lambda_p)N_1}{h(c/\lambda_p)A_{core}}\right) P_p + \left(\frac{\sigma^a(\lambda_k)}{h(c/\lambda_k)A_{core}}\right) N_1 P. \tag{2}$$

The first right-hand term in (2) represents spontaneous decay. The second one accounts for stimulated decay. Both terms are associated, respectively, with spontaneous and stimulated emissions of photons. The last two terms are associated, respectively, with the absorption of photons of P_p (excitation by the pump) and of the generated P (reabsorption). Reabsorption (the last term) is usually much smaller than excitation by the pump, because P is usually orders of magnitude smaller than P_p and because $\sigma^a(\lambda_p)$ is large. The spontaneous lifetime of the dopant in PMMA is represented as τ. Its value is about 0.3 ns for PFO and 2.85 ns for rhodamine B [18], [19]. A_{core} is the cross section of the fiber core, and h is Planck's constant.

For each subinterval centered at λ_k, the equation to calculate the evolution of P is

$$\frac{\partial P}{\partial z} = \sigma^e(\lambda_k)N_2P - \sigma^a(\lambda_k)N_1P - \frac{1}{c/n}\frac{\partial P}{\partial t} + \frac{N_2}{\tau}\left(h\frac{c}{\lambda_k}\right)\sigma^e_{sp}(\lambda_k)\beta A_{core}. \tag{3}$$

The first right-hand term in (3) accounts for the emission stimulated by an incoming photon. The second term represents the attenuation due to material absorption. The third term represents the propagation of the power inside the fiber with speed c/n. The spectral dependence of n is well approximated by an empirical formula reported for PMMA [20], which is basically the material employed to make the fiber core. The last term accounts for the spontaneous emissions associated with the spontaneous decays in (2). These are proportional to N_2/τ, and $\sigma^e_{sp}(\lambda_k)$ is the probability of spontaneous emissions at each subinterval. Since the direction of spontaneous photons is random, only a fraction β will be guided along the fiber. For a fiber of numerical aperture NA, we estimate the maximum value of β as the fraction of power emitted in all directions that is guided inside the fiber. This is an upper bound because not all the spontaneous electronic transitions produce photons. For example, for $NA = 0.5$ and $n = 1.492$, we have $\beta < NA^2/(4n^2) = 0.028$. Above threshold, the last term in (3), corresponding to spontaneous emissions, tends to be much smaller than the term corresponding to stimulated emissions. However, the former is necessary to simulate the appearance of the first photons in a laser. Note that we have neglected the possible occurrence of excited-state absorption of the pump power. The reason is that this phenomenon, which could be important for other applications [21], can be neglected for our type of analysis to a first approach [16]. Besides, in our model, we do not include possible nonlinear-absorption effects that could occur at very high power densities, such as the absorption of more than one photon simultaneously or via a multistep process, or the decrease in absorption due to optical saturation or optical bleaching. Such effects would require changing the equations described above. In addition, in the experimental works that we will use in Section 3, the authors did not report any of such nonlinear effects in their measurements.

The aforementioned equations are solved for the following initial conditions: P and N_2 are 0 at $t = 0$. We assume that a Gaussian pulse of pump power is launched into the fiber at $z = 0$ in the absence of input signal. Its temporal FWHM is short. We have taken 5 ns in the case of rhodamine-B doped fibers, which coincides with the conditions of the experimental results discussed in Section 3, and 0.1 ns in the case of PFO-doped ones. Anyway, we have seen, both computationally and experimentally, that an increase in the pulsewidth would not have a significant influence on the qualitative spectral behavior of the active fiber. The only requirement is that the value of the peak power should be reduced conveniently to keep the amount of pump energy constant. Regarding the light launching conditions, the same qualitative behavior can be expected if the illumination were applied laterally from the fiber side, provided that the length of the illuminated area was short enough. The main requirement is that the traveled distance in the fiber has to coincide. For the spectral analysis (e.g., for the calculation of λ_{av}, λ_{peak}, and FWHM as functions of z), the powers in the results will represent the time integrated powers, i.e., $P(z, \lambda_k) = \int_0^\infty P(t, z, \lambda_k)dt$.

The numerical approach used to solve the governing equations relies on finite differences. Specifically, we have developed ad-hoc finite-difference algorithms in which all three variables z, t, and λ have been discretized. The discretization of the spatial and temporal variables is uniform, i.e., with constant finite step sizes δt and δz. For example, for a distance of 7 cm and a pulsewidth of 5 ns, δz is on the order of $600 \cdot 10^{-9}$ m, δt is on the order of $0.2 \cdot 10^{-9}$ s, and roughly 8000 spatial

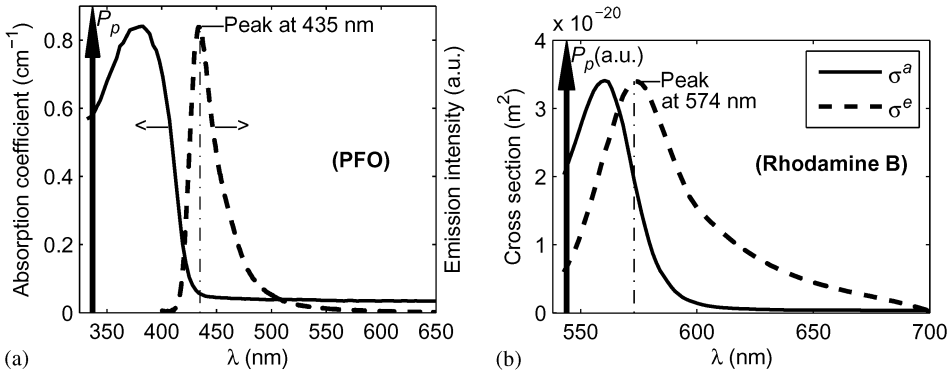

Fig. 3. Emission and absorption spectra of (a) PFO and (b) rhodamine B when used in PMMA. The emission spectra correspond to a very short length of doped PMMA POF (about 1 mm) in order for the absorption not to influence the measurements. The vertical arrow indicates the typical spectral location of the pump power P_p in each case.

nodes with 200 temporal steps are used. For smaller pulsewidths, δt is reduced. The judicious choice of these parameters is critical in order to achieve numerical convergence within the desired precision.

On the other hand, the discretization of λ has been carried out by dividing the full wavelength spectrum into three areas, each one with its own step size $\delta\lambda$. The first one, with a rather large value of $\delta\lambda$, starts at the pump wavelength ($\lambda_p = 543$ nm in the case of rhodamine-B doped fibers and $\lambda_p = 337$ nm in the case of PFO-doped ones). No photons with higher energies than those will come to exist in the system. The first coarse area extends up to some wavelength where the emission spectrum starts to be important. Next, a finely discretized section is used (with small $\delta\lambda$, on the order of 3 nm in our computations). Finally, a third section, again with coarse subintervals, can be used to take care of the low part of the right tail of the emission spectrum. The overall number of fine subintervals employed has been 50 in most of our calculations.

As for the implementation of the numerical scheme described, a few programming details follow. A matrix $\mathtt{N2(i,j)}$ is allocated to contain the discrete values of N_2, where index $\mathtt{i}$ determines t by $t_i = (\mathtt{i}-1)\delta t$ and index $\mathtt{j}$ determines z by $z_j = (\mathtt{j}-1)\delta z$. Similarly, a 3-D matrix $\mathtt{P(i,j,k)}$ is allocated in order to contain the light power distribution, where indices $\mathtt{i}$, $\mathtt{j}$ are as above, and index $\mathtt{k}$ determines λ according to the non-uniform discretization described. Finally, each term of the governing equations is estimated by means of finite differences for each discrete wavelength. The differences are centered whenever possible to achieve a higher order of precision. Both matrices $\mathtt{P(i,j,k)}$ and $\mathtt{N2(i,j)}$ are filled column by column. Columns represent values of z and rows represent values of t. A full column is calculated before going on to the next one.

3. Dye-Doped POF Parameters Derived Experimentally

Before discussing the results obtained computationally in the way explained above, let us consider some experimental results corresponding to fibers doped with PFO and rhodamine B.

In Fig. 3(a) and (b), we have plotted the emission and absorption spectra of both types of fibers. The graph in Fig. 3(a) was determined experimentally by us [3], whereas the necessary data to plot Fig. 3(b) can be found in several papers [6], [7], [17].

Fig. 4(a) and (b) reproduces some experimental studies already published by our group and collaborators [3] about the fluorescence of a PFO-doped POF below threshold for several distances z traveled by the light along the active fiber. As can be seen in Fig. 4(a), λ_{peak} did not change significantly in the range of distances measured, but the average wavelength changed quite linearly in about 7 nm along 6 cm of fiber, as shown in Fig. 4(b). The concentration of PFO used for the measurements was 0.003 wt%, which is close to the maximum that can be dissolved in PMMA. The pump power was below threshold (a pulsed nitrogen laser was employed with a pulsewidth of 4 ns, leading to a pulse energy on the order of 1 μJ/mm^2 at the entrance to the POF). Let us consider

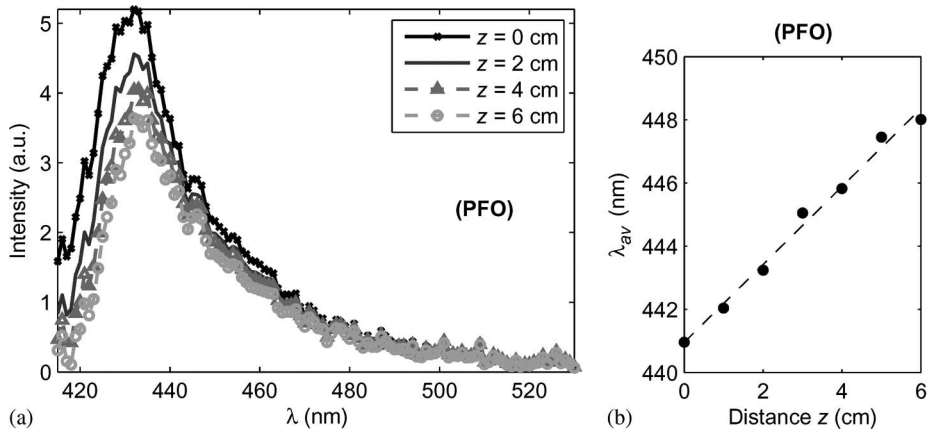

Fig. 4. Fluorescence red shifts in a PFO-doped PMMA POF for a concentration of PFO that is close to the maximum that can be dissolved in PMMA. (a) Spectra for different fiber distances, showing that the peak of the spectrum does not shift significantly. (b) Shift of λ_{av} as a function of fiber length. $\lambda_{av} = \int_{-\infty}^{\infty} \lambda P(\lambda) d\lambda / \int_{-\infty}^{\infty} P(\lambda) d\lambda$.

the behavior of the FWHM as a function of z. In PFO-doped POFs below threshold, the variations measured in the FWHM were very small and did not follow a clear tendency, as seen in Fig. 4(a). As for rhodamine-B doped POFs below threshold, from [17] we know that the red shift of the spectrum is much larger. Specifically, the authors report experimental results in very thin multimode core POFs (i.e., without cladding) drawn by them with concentrations of rhodamine B of 10^{-4}, 0.001 and 0.002 mol% (the latter could not be completely dissolved, as they explain). For such concentrations, they launched pulses of 5 ns with maximum pump power of 5 mW, i.e., clearly below threshold. Their results in distances up to 5 cm showed a continuous red shift in $\lambda_{peak}(z)$. Moreover, when the concentration was close to the maximum that could be dissolved (specifically, 0.001 mol%), the slope of $\lambda_{peak}(z)$ was not constant, since it was greater at the beginning and it clearly diminished when the distance z became greater than 3 cm. From 0.65 to 3 cm, $\lambda_{peak}(z)$ increased from about 605 to nearly 625 nm, as can be shown in the fourth figure of their paper [17]. Such experimental results about rhodamine B and ours about PFO show that there is a much greater red shift of the fluorescence below threshold in the case of rhodamine B. This effect can be explained by taking into account that the greater the degree of overlap is, the more influential the absorption becomes on the spectral power distribution. This is because its maximum tends to separate at low pump powers from the maximum of the emission curve $\sigma^e(\lambda)$ toward wavelengths of smaller attenuation. In the next section, we will gain insight into the influence of the overlap.

In some cases, a relative blue shift has been observed in the emitted power instead of a red one, but always at sufficiently high pump powers, which can be explained as follows. At the peak wavelength of the emission band the absorption is higher than that at longer wavelengths. This fact can be compensated above threshold by the greater probability of emissions as the light power increases with distance. Therefore, if the pump power is high enough for the distance considered, a relative blue shift with distance of λ_{peak} and of λ_{av} toward the peak of the cross section can be expected. The experimental corroboration of this shift can be found in the literature in the case of rhodamine-doped fibers [8], in a rhodamine dye solution embedded with nanoparticles [22], and in solid-state dyes [23]. The relative blue shift has not been reported yet in the case of PFO-doped fibers, as far as we know.

4. Computational Results and Discussion

First, let us analyze the red shift of the spectrum below threshold for the same dopant concentrations and similar initial pump energies as those commented in the previous section. Fig. 5(a) illustrates the evolution of λ_{av} with z for two different initial energies E_p of the launched pump pulse.

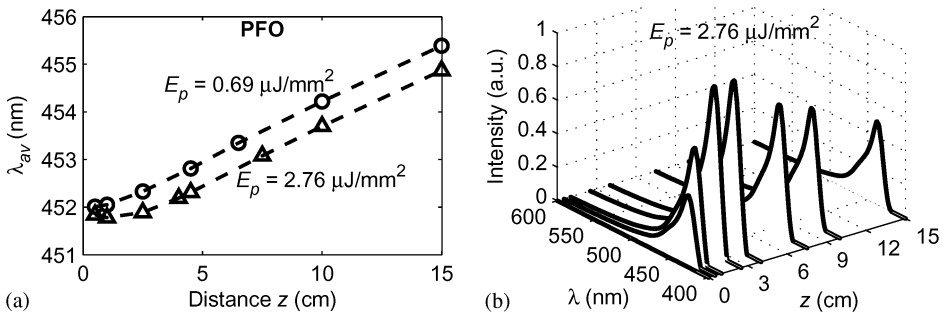

Fig. 5. (a) Average wavelength as a function of fiber length for PFO-doped fibers. The pump energy densities are inset. The concentration is 0.003 wt%. (b) Corresponding shapes of the emission spectra illustrating that the energy is below threshold.

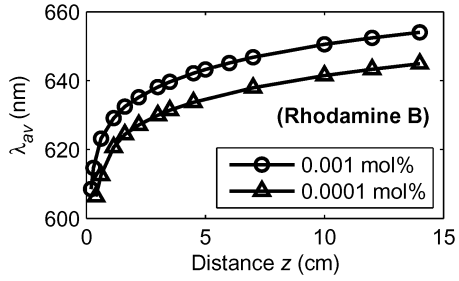

Fig. 6. Average output wavelength as a function of fiber length for rhodamine-B doped fibers. Pump pulse energy density is 8 μJ/mm^2. Dye concentrations are inset. A red shift in output spectrum is apparent.

In general, the linear behavior of $\lambda_{av}(z)$ agrees with the experimental results [see Fig. 4(b)]. The discrepancies in the values could be due to the differences in the distance traveled by the light in the fiber, which is longer in the case of the experimental results due to the measuring technique. In Fig. 5(a), an initial energy per unit area of 0.69 μJ/mm^2 yields a rather linear red shift of $\lambda_{av}(z)$ for distances longer than 1 cm. However, the linearity begins at a greater distance $(z \approx 3$ cm$)$ when $E_p = 2.76$ μJ/mm^2. This fact can be understood by observing the evolution of the generated power $P(z)$ in the latter case, which is illustrated in Fig. 5(b). This shows that the power grows until $z \approx 3$ cm is reached, since the launched energy is greater than in the other case. As we can see in Fig. 5(a), in both cases, there is a significant red shift of λ_{av}. This can be explained by taking into account that the absorption cross section decreases toward longer wavelengths in such a way that the decrease in the rate of absorptions is faster than that of emissions as wavelength increases. This effect is possible due to the overlap between the emission and absorption spectra. We have also corroborated that the red shift of the peak wavelength (λ_{peak}) is small in the case of PFO (we have obtained approximately 1.5 nm of red shift in the first 15 cm of fiber).

Fig. 6 shows that the red shift below threshold obtained for rhodamine-B doped POFs is much greater. In this case, the red shift of λ_{av} in a distance of 14.5 cm, from $z = 0.5$ cm to $z = 15$ cm, is greater than 40 nm, i.e., roughly one order of magnitude greater than in the case of PFO. Moreover, when rhodamine B is used there is a great shift even in λ_{peak}, since it changes from being 600 nm at $z = 0.5$ cm to being nearly 640 nm at $z = 14$ cm when the concentration is 0.0001 mol%. The red shift grows initially faster when the concentration is greater [as shown in Fig. 7(b)]. For the sake of comparison between the shifts in λ_{peak} for both types of doped fibers, the corresponding curves are shown in Fig. 7(a) and (b). It is clear from the results obtained that, in the case of rhodamine B, the slope of the shift of $\lambda_{av}(z)$ or of $\lambda_{peak}(z)$ is not constant. It is greater at the beginning, coinciding with a very large overlap between the spectrum of P and the absorption curve. This is because P is not yet very red-shifted when z is small. The fact that the red shift is greater when the concentration of

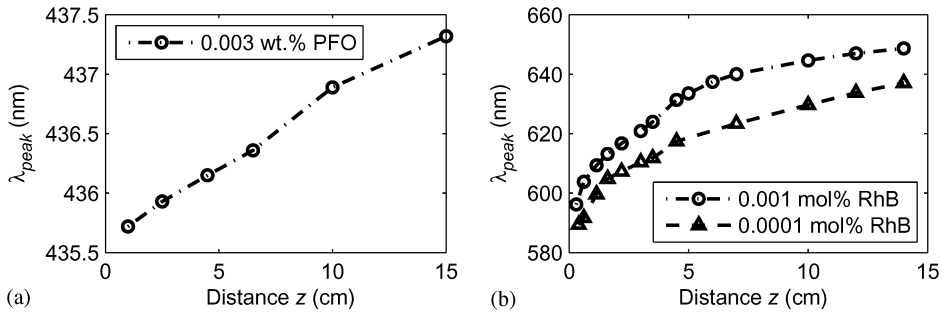

Fig. 7. (a) Peak wavelength as a function of fiber length for PFO-doped fibers. Pump pulse energy density is 0.69 μJ/mm^2. Dye concentration is inset. The peak remains close to 435 nm. (b) Corresponding plots for rhodamine-B doped fibers under the same conditions as in Fig. 6 (8 μJ/mm^2), showing that the shift is much larger than in (a).

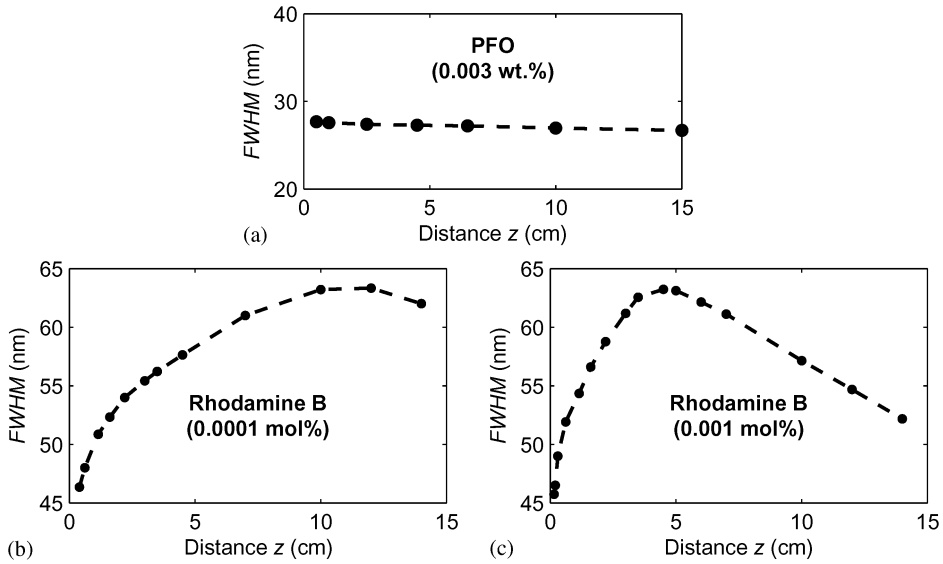

Fig. 8. Full width at half maximum as a function of fiber length for (a) PFO and (b) and (c) rhodamine B. The pump energies are well below threshold: 0.69 μJ/mm^2 for PFO and 8 μJ/mm^2 for rhodamine B.

rhodamine B is 0.001 mol% than when it is 0.0001 mol% [see Fig. 7(b)] can be explained by noting that the attenuation is higher in the former case. This increases the importance of the shape of the absorption spectrum that overlaps with the emission spectrum [24].

Let us now analyze the behavior of the spectral widths. Specifically, when the pump energy is well below threshold, there can be an initial increase in the FWHM followed by a decrease, as shown in Fig. 8 for PFO and rhodamine B. The threshold pump energy density depends on the fiber length, on the type of dopant and on the concentration. In the case of the POF doped with PFO, we saw in Fig. 5 that an energy in the order of 0.7 μJ/mm^2 was below threshold for a few centimeters of distance, since the two pump energy densities employed in Fig. 5(a) (0.69 and 2.76 μJ/mm^2) were below threshold in such conditions. In the case of the POF doped with rhodamine B, a value of 8 μJ/mm^2 is below threshold for the distances considered in Fig. 8, as was commented in Section 3 [17]. Fig. 8(a) shows that the change of the FWHM in the case of PFO is small in the range of distances from 0.5 to 15 cm, which agrees with the experimental results of Section 3. In the case of a rhodamine-B doped fiber, the great variations in the attenuations of individual wavelengths when the spectrum is not red shifted very much produce an initial increase of the width with distance. Simultaneously, a red shift of the average wavelength occurs. This effect is especially influential at the beginning, when the

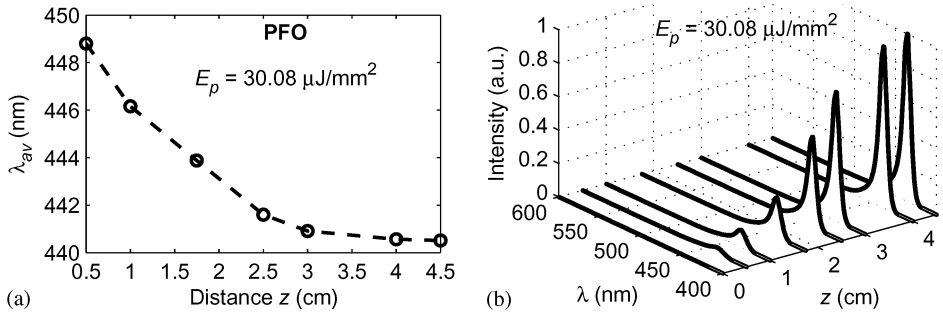

Fig. 9. (a) Average wavelength as a function of fiber length for PFO-doped fibers. Pump pulse energy density is inset. Dye concentration is 0.003 wt%. (b) Corresponding shapes of the emission spectra illustrating that the energy is above threshold.

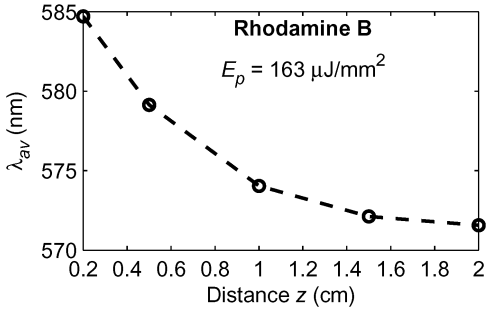

Fig. 10. Average wavelength in the case of a rhodamine-B doped POF when the concentration is 0.0001 mol% for a pump energy above threshold.

overlap between the spectrum of the emitted light and the absorption cross sections is greater, which explains the initial increase of the FWHM with distance (see Fig. 8(b) and (c), corresponding to two different concentrations).

Let us now consider what happens when pumping the fiber above threshold. When the pump power intensity is sufficiently high, there can be a greater net gain (gain minus absorption) at shorter wavelengths than at longer ones in a large part of the range of emitted wavelengths. Therefore, a relative blue shift of $\lambda_{av}(z)$ can occur. This effect is shown in Fig. 9(a) in the case of a PFO-doped fiber. The pump energy employed is shown to be above threshold in Fig. 9(b), which shows the narrowing of the emission spectra as z increases up to 4.5 cm, which is the length of maximum gain.

The relative blue shift above threshold also appears in the case of rhodamine-B doped fibers, as shown in Fig. 10, which corresponds to a concentration of 0.0001 mol%. In this case, the high attenuation of the fiber is much higher than in the case of a POF strongly doped with PFO; therefore, the energy pulse has been higher in order to be above threshold. The slope of $\lambda_{av}(z)$ tends to reduce as the length of maximum gain is approached. It can be observed that, for $z > 1$ cm, λ_{av} takes values that are slightly below 574 nm (peak wavelength of the emission cross section of rhodamine B). This unexpected behavior could not be easily explained if the absorption cross section always decreased with λ. However, σ^a increases for λ from $\lambda_p = 540$ nm up to 561 nm, which tends to reduce λ_{av}. Apart from that, discretization errors in the numerical method employed, as well as the simplifying hypotheses assumed, could also contribute to this effect.

Regarding the evolution of the FWHM with distance, we can see that it decreases with a slope that tends to 0 as the length of maximum gain is approached, as can be seen in Fig. 11. The narrowing of the FWHM has also been observed when z is constant and the pump power is increased above threshold, but that is a well-known effect [25].

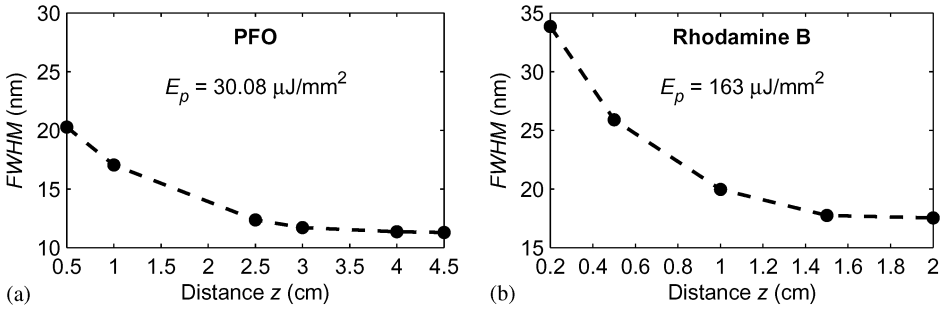

Fig. 11. Evolution of the FWHM with distance for POFs doped with (a) PFO and (b) rhodamine B when the pump energies are above threshold. The concentrations are 0.003 wt% and 0.0001 mol%, respectively. The energy densities pumped are inset.

5. Conclusion

In this work, we have computationally analyzed the spectral features of light power in doped POFs. For this purpose, we have developed ad-hoc numerical algorithms. We have taken two representative cases regarding the overlap between absorption and emission: fibers doped with PFO and fibers doped with rhodamine B. There are shifts along the fiber of the emission spectra toward longer or shorter wavelengths when the pump power is below or above threshold, respectively. These shifts are greater in the case of larger cross section overlaps. As for the spectral width of the emission, its evolution with the fiber length depends on the pump power and on the type of dopant employed. Above threshold there is an initial decrease with distance in the FWHM in both cases. These analyses can be very useful to develop tunable POF-based optical amplifiers and lasers.

Acknowledgment

Two of the authors have research fellowships from Vicerrectorado de Euskara y Plurilingüismo, UPV/EHU, and from Vicerrectorado de Investigación, UPV/EHU, while working on their Ph.D. degrees.

References

[1] G. V. Maier, T. N. Kopylova, V. A. Svetlichnyi, V. M. Podgaetskii, S. M. Dolotov, O. V. Ponomareva, A. E. Monich, and E. A. Monich, "Active polymer fibres doped with organic dyes: Generation and amplification of coherent radiation," *Quantum Electron.*, vol. 37, no. 1, pp. 53–59, 2007.

[2] M. Sheeba, K. J. Thomas, M. Rajesh, V. P. N. Nampoori, C. P. G. Vallabhan, and P. Radhakrishnan, "Multimode laser emission from dye doped polymer optical fiber," *Appl. Opt.*, vol. 46, no. 33, pp. 8089–8094, Nov. 2007.

[3] M. A. Illarramendi, J. Zubia, L. Bazzana, G. Durana, G. Aldabaldetreku, and J. R. Sarasua, "Spectroscopic characterization of plastic optical fibers doped with fluorene oligomers," *J. Lightwave Technol.*, vol. 27, no. 15, pp. 3220–3226, Aug. 2009.

[4] J. Zubia and J. Arrue, "Plastic optical fibers: An introduction to their technological processes and applications," *Opt. Fiber Technol.*, vol. 7, no. 2, pp. 101–140, Apr. 2001.

[5] J. Clark, L. Bazzana, D. D. C. Bradley, J. Cabanillas-Gonzalez, G. Lanzani, D. G. Lidzey, J. Morgado, A. Nocivelli, W. C. Tsoi, T. Virgili, and R. Xia, "Blue polymer optical fiber amplifiers based on conjugated fluorine oligomers," *J. Nanophoton.*, vol. 2, p. 023504, 2008.

[6] H. Liang, Z. Zheng, Z. Li, J. Xu, B. Chen, H. Zhao, and Q. Zhang, "Fabrication and amplification of rhodamine B-doped step-index polymer optical fiber," *J. Appl. Polym. Sci.*, vol. 93, no. 2, pp. 681–685, 2004.

[7] G. D. Peng, P. L. Chu, Z. Xiong, T. W. Whitbread, and R. P. Chaplin, "Dye-doped step-index polymer optical fiber for broadband optical amplification," *J. Lightwave Technol.*, vol. 14, no. 10, pp. 2215–2223, Oct. 1996.

[8] M. Rajesh, M. Sheeba, K. Geetha, C. P. G. Vallaban, P. Radhakrishnan, and V. P. N. Nampoori, "Fabrication and characterization of dye-doped polymer optical fiber as a light amplifier," *Appl. Opt.*, vol. 46, no. 1, pp. 106–112, Jan. 2007.

[9] J. R. Lawrence, G. A. Turnbull, and I. D. W. Samuel, "Broadband optical amplifier based on a conjugated polymer," *Appl. Phys. Lett.*, vol. 80, no. 17, pp. 3036–3038, Apr. 2002.

[10] A. Tagaya, S. Teramoto, E. Nihei, K. Sasaki, and Y. Koike, "High-power and high-gain organic dye-doped polymer optical fiber amplifiers: Novel techniques for preparation and spectral investigation," *Appl. Opt.*, vol. 36, no. 3, pp. 572–578, 1997.

[11] A. Tagaya, Y. Koike, E. Nihei, S. Teramoto, K. Fujii, T. Yamamoto, and K. Sasaki, "Basic performance of an organic dye-doped polymer optical fiber amplifier," *Appl. Opt.*, vol. 34, no. 6, pp. 988–992, 1995.
[12] K. Geetha, M. Rajesh, V. P. N. Nampoori, C. P. G. Vallabhan, and P. Radhakrishnan, "Loss characterization in rhodamine 6G doped polymer film waveguide by side illumination fluorescence," *J. Opt. A, Pure Appl. Opt.*, vol. 6, no. 4, pp. 379–383, Feb. 2004.
[13] I. D. W. Samuel, E. B. Namdas, and G. A. Turnbull, "How to recognize lasing," *Nat. Photon.*, vol. 3, no. 10, pp. 546–549, Oct. 2009.
[14] U. Scherf, S. Riechel, U. Lemmerb, and R. F. Mahrtc, "Conjugated polymers: Lasing and stimulated emission," *Curr. Opinion Solid State Mater. Sci.*, vol. 5, no. 2/3, pp. 143–154, Apr.–Jun. 2001.
[15] D. Amarasinghe, A. Ruseckas, G. A. Turnbull, and I. D. W. Samuel, "Organic semiconductor optical amplifiers," *Proc. IEEE*, vol. 97, no. 9, pp. 1637–1650, Aug. 2009.
[16] A. Tagaya, S. Teramoto, T. Yamamoto, K. Fujii, E. Nihei, Y. Koike, and K. Sasaki, "Theoretical and experimental investigation of rhodamine B-doped polymer optical fiber amplifiers," *IEEE J. Quantum Electron.*, vol. 31, no. 12, pp. 2215–2219, Dec. 1995.
[17] E. De La Rosa-Cruz, C. W. Dirk, O. Rodríguez, and V. M. Castaño, "Characterization of fluorescence induced by side illumination of rhodamine B doped plastic optical fibers," *Fiber Integr. Opt.*, vol. 20, no. 5, pp. 457–464, Sep. 2001.
[18] R. Xia, G. Heliotis, Y. Hou, and D. D. C. Braddley, "Fluorene-based conjugated polymer optical gain media," *Organ. Electron.*, vol. 4, no. 2/3, pp. 165–177, Sep. 2003.
[19] M. Karimi, N. Granpayeh, and M. K. M. Farshi, "Analysis and design of a dye-doped polymer optical amplifier," *Appl. Phys. B, Photophys. Laser Chem.*, vol. 78, no. 3/4, pp. 387–396, Feb. 2004.
[20] C. Gao and G. Farrell, "Modelling of Rayleigh backscattering in plastic optical fiber," in *Proc. High Freq. Postgraduate Student Colloq.*, 2003, pp. 14–17.
[21] S. Speiser and N. Shakkour, "Photoquenching parameters for commonly used laser dyes," *Appl. Phys. B, Photophys. Laser Chem.*, vol. 38, no. 3, pp. 191–197, Nov. 1985.
[22] H. Z. Wang, F. L. Zhao, Y. J. He, X. G. Zheng, X. G. Huang, and M. M. Wu, "Low-threshold lasing of a rhodamine dye solution embedded with nanoparticle fractal aggregates," *Opt. Lett.*, vol. 23, no. 10, pp. 777–779, May 1998.
[23] S. Y. Lam and M. J. Damzen, "Characterisation of solid-state dyes and their use as tunable laser amplifiers," *Appl. Phys. B, Photophys. Laser Chem.*, vol. 77, no. 6/7, pp. 577–584, 2004.
[24] A. Kuriain, N. A. George, B. Paul, V. P. N. Nampoori, and C. P. G. Vallabhan, "Studies on fluorescence efficiency and photodegradation of rhodamine 6G doped PMMA using a dual beam thermal lens technique," *Laser Chem.*, vol. 20, no. 2–4, pp. 99–110, Jan. 2002.
[25] C. J. Koester and E. Snitzer, "Amplification in a fiber laser," *Appl. Opt.*, vol. 3, no. 10, pp. 1182–1186, Oct. 1964.